Received: 12 February 2021 | Revised: 5 June 2021 | Accepted: 8 June 2021

DOI: 10.1096/fj.202100262RR

RESEARCH ARTICLE

THE FASEB JOURNAL

Allostatic hypermetabolic response in PGC1α/β heterozygote mouse despite mitochondrial defects

Sergio Rodriguez-Cuenca[1] | Christopher J. Lelliot[2] | Mark Campbell[1] | Gopal Peddinti[3] | Maite Martinez-Uña[4] | Camilla Ingvorsen[1] | Ana Rita Dias[1] | Joana Relat[5,6] | Silvia Mora[7] | Tuulia Hyötyläinen[8] | Antonio Zorzano[9,10,11] | Matej Orešič[8,12] | Mikael Bjursell[2] | Mohammad Bohlooly-Y[2] | Daniel Lindén[13,14] | Antonio Vidal-Puig[1,15]

[1]Wellcome-MRC Institute of Metabolic Science, University of Cambridge, Cambridge, UK

[2]Discovery Sciences, BioPharmaceuticals R&D, AstraZeneca, Gothenburg, Sweden

[3]VTT, Technical Research Center of Finland, Espoo, Finland

[4]Department of Physiology, University of the Basque Country UPV/EHU, Bilbao, Spain

[5]Department of Nutrition, Food Science and Gastronomy, School of Pharmacy and Food Science, Food and Nutrition Torribera Campus, University of Barcelona (UB), Santa Coloma de Gramenet, Spain

[6]INSA-UB, Nutrition and Food Safety Research Institute, University of Barcelona, Barcelona, Spain

[7]Department of Cellular and Molecular Physiology, Institute of Translational Medicine, The University of Liverpool, Liverpool, UK

[8]School of Science and Technology, Örebro University, Örebro, Sweden

[9]Institute for Research in Biomedicine (IRB Barcelona), The Barcelona Institute of Science and Technology, Barcelona, Spain

[10]Dept. Biochemistry and Molecular Biomedicine, University of Barcelona, Barcelona, Spain

[11]Centro de Investigación Biomédica en Red de Diabetes y Enfermedades Metabólicas Asociadas (CIBERDEM), Instituto de Salud Carlos III, Madrid, Spain

[12]Turku Bioscience Centre, University of Turku and Åbo Akademi University, Turku, Finland

[13]Research and Early Development Cardiovascular, Renal and Metabolism, BioPharmaceuticals R&D, AstraZeneca, Gothenburg, Sweden

[14]Division of Endocrinology, Department of Neuroscience and Physiology, Sahlgrenska Academy, University of Gothenburg, Gothenburg, Sweden

[15]Wellcome Trust Sanger Institute, Wellcome Trust Genome Campus, Hinxton, UK

Correspondence
Sergio Rodriguez-Cuenca, Wellcome-MRC Institute of Metabolic Science, University of Cambridge, Cambridge, UK.
Email: sr441@medschl.cam.ac.uk

Daniel Lindén, Research and Early Development Cardiovascular, Renal and Metabolism, BioPharmaceuticals R&D, AstraZeneca, Gothenburg, Sweden.
Email: daniel.linden@astrazeneca.com

Abstract

Aging, obesity, and insulin resistance are associated with low levels of PGC1α and PGC1β coactivators and defective mitochondrial function. We studied mice deficient for PGC1α and PGC1β [double heterozygous (DH)] to investigate their combined pathogenic contribution. Contrary to our hypothesis, DH mice were leaner, had increased energy dissipation, a pro-thermogenic profile in BAT and WAT, and improved carbohydrate metabolism compared to wild types. WAT showed upregulation

Abbreviations: AALAC, the association for assessment and accreditation of laboratory animal care international; BAT, brown adipose tissue; DAG, diacylglycerol; DH, double heterozygote; FAO, fatty acid oxidation; FDR, false discovery rate; GTT, glucose tolerance test; HET, heterozygote; HFD, high fat diet; KO, knock-out; mt-OXPHOS, mitochondrial encoded oxidative phosphorylation machinery; nt- OXPHOS, nuclear encoded oxidative phosphorylation machinery; PC, phosphatidylcholine; PCR, polymerase chain reaction; PE, phosphatidylethanolamine; PGC1, peroxisome proliferator-activated receptor gamma coactivator 1; RER, respiratory exchange ratio; RT, room temperature; SM, sphingomyelin; TG, triacylglycerol; WAT, white adipose tissue; WT, wild type.

Present address
Christopher J. Lelliot, Wellcome-MRC Institute of Metabolic Science, University of Cambridge, Cambridge, UK
Gopal Peddinti, University of Turku, Turku, Finland
Maite Martinez-Uña, Madrid Institute for Advanced Studies, Madrid, Spain
Camilla Ingvorsen, Novo Nordisk, Copenhagen, Denmark
Silvia Mora, Dept. Biochemistry and Molecular Biomedicine, University of Barcelona, Barcelona, Spain

Funding information
EC | FP7 | FP7 Health (HEALTH), Grant/Award Number: [HEALTH-F4-2008-223450; RCUK | Medical Research Council (MRC), Grant/Award Number: MC_UU_12012/2 and MC_UU_00014/5; European Commission (EC), Grant/Award Number: MEIF-CT-2005-023061; Wellcome Trust (Wellcome), Grant/Award Number: 208363/Z/17/Z

of mitochondriogenesis/oxphos machinery upon allelic compensation of PGC1α4 from the remaining allele. However, DH mice had decreased mitochondrial OXPHOS and biogenesis transcriptomes in mitochondria-rich organs. Despite being metabolically healthy, mitochondrial defects in DH mice impaired muscle fiber remodeling and caused qualitative changes in the hepatic lipidome. Our data evidence first the existence of organ-specific compensatory allostatic mechanisms are robust enough to drive an unexpected phenotype. Second, optimization of adipose tissue bioenergetics is sufficient to maintain a healthy metabolic phenotype despite a broad severe mitochondrial dysfunction in other relevant metabolic organs. Third, the decrease in PGC1s in adipose tissue of obese and diabetic patients is in contrast with the robustness of the compensatory upregulation in the adipose of the DH mice.

KEYWORDS
adipose tissue, hepatic lipidome, lipotoxicity, mitochondrial dysfunction, PGC-1alpha

1 | INTRODUCTION

Obesity and associated metabolic complications worsen with age. Moreover, the metabolic stress induced by overnutrition, obesity, and diabetes accelerates the decay of aging through mechanisms that remain poorly understood. Aging, per se, is associated with downregulation of mitochondrial oxidative phosphorylation machinery (OXPHOS), mitochondriogenesis program, and β-oxidation genes. Mitochondrial malfunction and overproduction of ROS are pathogenically relevant for insulin resistance, β-cell dysfunction, and impaired glucose tolerance. Thus, we posited that bioenergetics failure and/or decay of mitochondrial fuel efficiency might pathogenically contribute to age and obesity-associated metabolic stress.

We and others have shown that PGC1α and PGC1β[1] control energy expenditure (EE), fatty acid oxidation (FAO) and the metabolic switch between lipid and glucose utilization.[2] PGC1α and PGC1β are essential regulators of mitochondriogenesis and antioxidant transcriptional program, although their functions do not overlap completely. PGC1β preferentially modulates hepatic lipid metabolism, de novo lipogenesis and secretion of triglycerides,[3] whereas PGC1α controls hepatic gluconeogenesis and cold-induced thermogenesis,[4] mitochondrial biogenesis, adaptation to fasting/caloric restriction and exercise. Several functional transcriptional variants for PGC1α with specific regulatory roles[5,6] exists, raising the prospect of independent nodes of control of the transcriptional regulation of the PGC1 family members.

GWAS have identified SNPs in PGC1α and PGC1β associated with increased risk for obesity, T2DM and NAFLD.[7-9] Several clinical studies have shown that expression of *PGC1α* and *PGC1β* is downregulated in the skeletal muscle of T2DM patients with impaired mitochondrial function.[10-12] Similarly, white adipose tissue (WAT) from obese, T2DM individuals[13-15] and offspring of gestational diabetic mothers exhibited decreased expression of *PGC1α*.[16,17] We have shown that human myocytes exposed to conditional media from adipocytes of obese subjects downregulate PGC1α and β mRNA expression.[18] Thus, the decrease in PGC1α and β may be secondary to the systemic inflammation associated with obesity and T2DM. These pieces of evidence raise the questions of whether dysfunctional PGC1α/PGC1β plays a causal role in the onset and development of T2DM and obesity or whether these changes are mere bystanders consequence of the severity of the associated metabolic disturbances.

Our initial hypothesis was that the combined decrease of PGC1α/PGC1β as observed in the elderly[19] and/or in obese and insulin-resistant patients[20] was a primary pathogenic mechanism leading to impaired mitochondrial function, defective fuel utilization, lipotoxicity and metabolic dysfunction. However, in retrospect, we should not have discarded the metabolic relevance of the allostatic adaptations maintaining the functionality of PGC1α protein levels. Global ablation of either *ppargc1a* or *ppargc1b* genes in mice is associated with over-expression of the non-targeted *ppargc1* mRNA in a tissue-dependent manner.[21-24] Thus, it is conceivable that the

dysfunction of one of the PGC1 variants may paradoxically provide an "initial" metabolic advantage as a result of a transient "allostatic compensation" from an a priori less relevant peripheral organ.

Here, we demonstrate that $pgc1\alpha^{[het]} \times pgc1\beta^{[het]}$ (DH) mice, despite exhibiting downregulation of mitochondrial function genes, they have a paradoxical increase in global EE, BAT activation and leanness, amelioration of carbohydrate metabolism particularly under chow diet, coincident with a compensatory regulation of *pgc1α4* expression in WAT. Notwithstanding this metabolic advantage, the DH mice exhibits defects in muscle remodeling and qualitative changes in the hepatic lipidome. These data highlight the existence of functionally relevant robust allostatic mechanisms in adipose tissue aimed to preserve protein levels of PGC1α in a model of global PGC1 double heterozygosity.

2 | MATERIAL AND METHODS

2.1 | Experimental animals

$pgc1\alpha^{[het]} \times pgc1\beta^{[het]}$ (DH) mice and wild-type (WT) littermates were generated after crossing heterozygous mice for either *pgc1α*[25] and *pgc1β*.[22]

Mice were housed in a temperature-controlled room with a 12-hours light/dark cycle. Food and water were available ad libitum. Littermate mice were fed a chow diet (D12450B) or HFD (60% Kcal) (D12492) for 23 weeks from weaning. The experimental procedures were approved by the Gothenburg ethics review committee on animal experiments and were following Swedish and European Union laws on the use and treatment of experimental animals. Animals were kept in a facility accredited by AAALAC.

2.2 | Real-time PCR

Real-Time PCR was performed in a 7900HT Fast Real-Time PCR System as described.[26] For all experiments, gene expression profiling was corrected by the geometric average of 18S, β2-microglobulin, β-actin, and 36B4. Heatmaps were generated using ClustVis (https://biit.cs.ut.ee/clustvis/).

2.3 | Western blotting

Protein lysates (150-200 μg) were run in an SDS-PAGE and transferred to a cellulose membrane using the iBlot system. A rabbit polyclonal against PGC1α from abcam (ab54481) was used as primary antibody.

2.4 | Blood biochemistry

3-OH Butyrate (Stanbio Beta Hydroxybutyrate Liquicolour), Free Fatty Acids (Roche). Triglycerides (Siemens Dimension RxL analyser) were measured according to the manufacturer's instructions.

2.5 | EE analysis

Indirect calorimetry was performed using an Oxymax Lab Animal Monitoring System (Columbus Ins). RER was calculated by using the cosinor method to estimate the mesor + amplitude of each RER curves.[27] Voluntary locomotor activity was measured as number of laser breaks/min.

2.6 | Carbohydrate metabolism

For oral glucose tolerance test (oGTT), mice were fasted for 4 hours before basal measurement of blood glucose, followed by oral gavage of a glucose bolus (2 g/kg). Blood glucose and insulin were measured at 0, 15, 30, 60, and 120 minutes after the bolus.

2.7 | Lipidomics

Lipid extracts were analyzed on a Q-ToF Premier mass spectrometer (Waters) combined with an Acquity Ultra Performance Liquid chromatography (UPLC/MS). The extracts were analyzed on an Acquity UPLCTM BEH C18 2.1 × 100 mm column packed with 1.7 μm particles.[28] Data were processed using MZmine 2 software.[29] All the identified lipids were quantified by normalizing with corresponding lipid class-specific internal standards.

2.8 | Imaging

Liver. Level of steatosis was assessed and manually curated by using HALO (Indica labs). *WAT/BAT*. Images were transformed into 8-bit type (gray) and processed as binary (B/W) using Cell-P (Olympus). For WAT, the size of the adipocytes was determined by measuring the area in μm^2. For BAT, the scores for intracellular vacuoles area in the analyzed field were calculated by dividing the target areas by the total BAT area.

2.9 | Statistical analysis

Differences in gene expression using two-way ANOVA were considered statistically significant at $P \leq .05$ and

$q \leq 0.05$ (FDR). Two-way ANOVA was also used for any other phenotypical analysis (SPSS-26). ANCOVA was used to adjust EE for differences in body weight.[30] For lipidomics we performed a dual analysis (a) an ANOVA of the sum of the different lipids to assess the quantitative impact on the lipidome and (b) a MANOVA followed by a two-way ANOVA or discriminant analysis when appropriate. Lipid ontology enrichment was performed using LION/Web.[31]

3 | RESULTS

3.1 | *Pgc1α*[het] × *Pgc1β*[het] mice are viable

PGC1α × PGC1β double heterozygotes were obtained at the expected mendelian ratio by crossing PGC1α and PGC1β double heterozygotes. No *Pgc1α*[ko] × *Pgc1β*[ko] were generated, confirming that lacking both PGC1s is not viable.[32] DH Mice were not dysmorphic, although their body weight at six weeks of age was lower than WT littermates (Figure 1A).

3.2 | *Pgc1α*[het] × *Pgc1β*[het] mice are lean and hypermetabolic

DH mice were leaner than their WT littermates, a phenotype that was more evident when fed on a chow diet (Figure 1B,C). A similar tendency, albeit not significant, was observed in HFD fed mice.

Indirect calorimetry analysis revealed higher EE in DH mice vs WT littermates when fed chow diet (Figure 1D). Locomotor activity tended to be lower in the chow-fed DH mice (ns) (Figure 1E). The higher RER value in DH mice revealed preferential oxidation of carbohydrates vs fat when fed chow diet, more evident during the night period (Figure 1F). In HFD-fed mice, no differences in RER or EE were observed between DH and WT mice. Globally, these data indicate that on chow diet, DH mice were hypermetabolic and exhibited preferential use of carbohydrates vs lipids as substrates. This phenotype was mitigated when mice were fed HFD. No differences in food intake were observed (not shown).

The insulin measurements collected following an oGTT revealed that chow-fed DH mice required less insulin to maintain normoglycemia when compared to WT mice (Figure 1G). A priori, this indicated that the DH mice were more insulin sensitive. On HFD, the DH mice exhibited similar glucose tolerance as WT with no differences in insulin levels.

Serum biochemistry revealed reduced triglycerides, but no changes in the levels of free fatty acids, ketone bodies, lactate and FGF21 in DH mice-fed chow vs WT (Figure 1H).

3.3 | *Pgc1α*[het] × *Pgc1β*[het] mice presented an increased thermogenic fingerprint in BAT despite impaired mitochondrial program

The BAT from chow-fed DH mice weighed less when compared to WT mice (data not shown). The histological analysis of BAT revealed increased multilocularity in the DH mice (Figure 2A,B). Levels of *pgc1β* mRNA in BAT were reduced by 40% in DH vs WT in both chow and HFD conditions (Figure 2C). At the protein level, PGC1α1 but not the PGC1α4 isoform was reduced in a genotype-dependent manner in both nutritional conditions (Figure 2D).

This finding matched with the decreased expression of mitochondrial OXPHOS genes and with the reduction of multiple genes responsible for mitochondrial fusion and fission (Figure 2E), indicating a general impairment in mitochondrial dynamics and performance. Of note, *lpgds* mRNA was downregulated in DH BAT (Figure 2E); in agreement with previous observation where the absence of LPGDS promoted the use of carbohydrates vs lipids in BAT[33] and exhibited higher RER in chow-fed DH mice. The transcriptional profiling of BAT in DH mice also revealed upregulation of pro-thermogenic genes such as *dio2* as well as *lpl, fatp1, cd36* and *aox* (Figure 2E). Upregulation of these genes is consistent with optimization of lipid uptake for mitochondrial and peroxisomal FAO[34]; whether this phenomenon is related to the concomitant upregulation observed for PGC1α2 and PGC1α3 mRNA (Figure 2C) is unknown.

3.4 | WAT from *Pgc1α*[het] × *Pgc1β*[het] mice had smaller adipocytes, allelic overcompensation of PGC1α variants, and increased expression of mtOXPHOS genes

Chow-fed DH mice had reduced fat % associated with a histological fingerprint characterized by smaller adipocytes in gonadal fat tissue (gWAT). A similar trend but less robust was observed in HFD fed mice (Figure 3A,B). This histological detail indicated that the lean phenotype in chow-fed DH mice was not the result of partial lipodystrophy but instead in the context of improved insulin sensitivity as a consequence of negative energy balance in chow-fed DH mice. This negative energy balance was mitigated when the mice were fed on HFD.

Gene expression analysis of gWAT revealed that both isoforms of *pgc1α* (α1 and α4) in DH mice were not downregulated as would have been expected from heterozygosity (Figure 3C). As expected *Pgc1β* mRNA levels were decreased in DH gWAT in chow and HFD (25% and 40%, respectively) (Figure 3C). At the protein level, the expression of PGC1α1 was stable, and surprisingly, the level of PGC1α4 protein was increased in DH (Figure 3D).

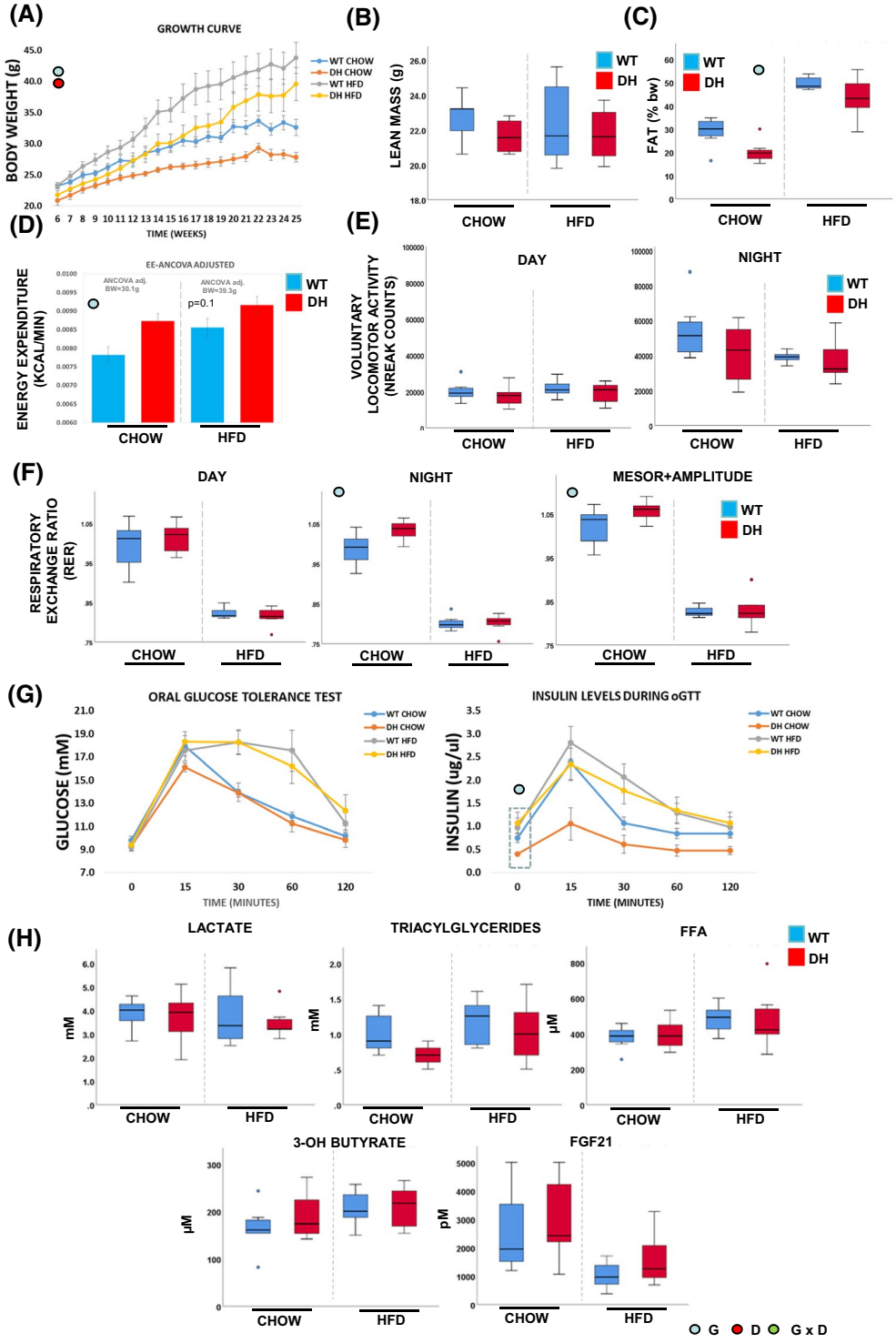

FIGURE 1 A, Growth curves of male DH and littermate WT mice are shown for chow-fed, and high-fat diet fed mice. B and C, Body lean mass and fat mass by DEXA at culling. D, Energy expenditure per mouse (kcal/min per mouse). E, Voluntary locomotor activity (laser breaks/min). F, RER at room temperature. G, Oral glucose tolerance test (oGTT) and Insulin measurement during oGTT in DH- and WT mice-fed chow or high-fat diet (HFD). H, Serum biochemistry. (n = 7-9 mice per genotype). Data presented as mean ± SEM. DH, $Pgc1\alpha^{[het]} \times Pgc1\beta^{[het]}$; WT, wild-type. *$P < .05$ by Two-way ANOVA

The paradoxical maintenance of the levels of *pgc1α1* and increase in *pgc1α4* was associated with and enrichment in mitochondrial encoded OXPHOS genes that clustered separately from nuclear DNA-encoded subunit genes (Figure 3E) such as mtATP8, mtCO2, mtND4 ($P \leq .05$, FDR ≤ 0.05), mtATP6, mtCO3, mtCYB, mtND5 ($P \leq .05$, FDR ≥ 0.05) as well as a

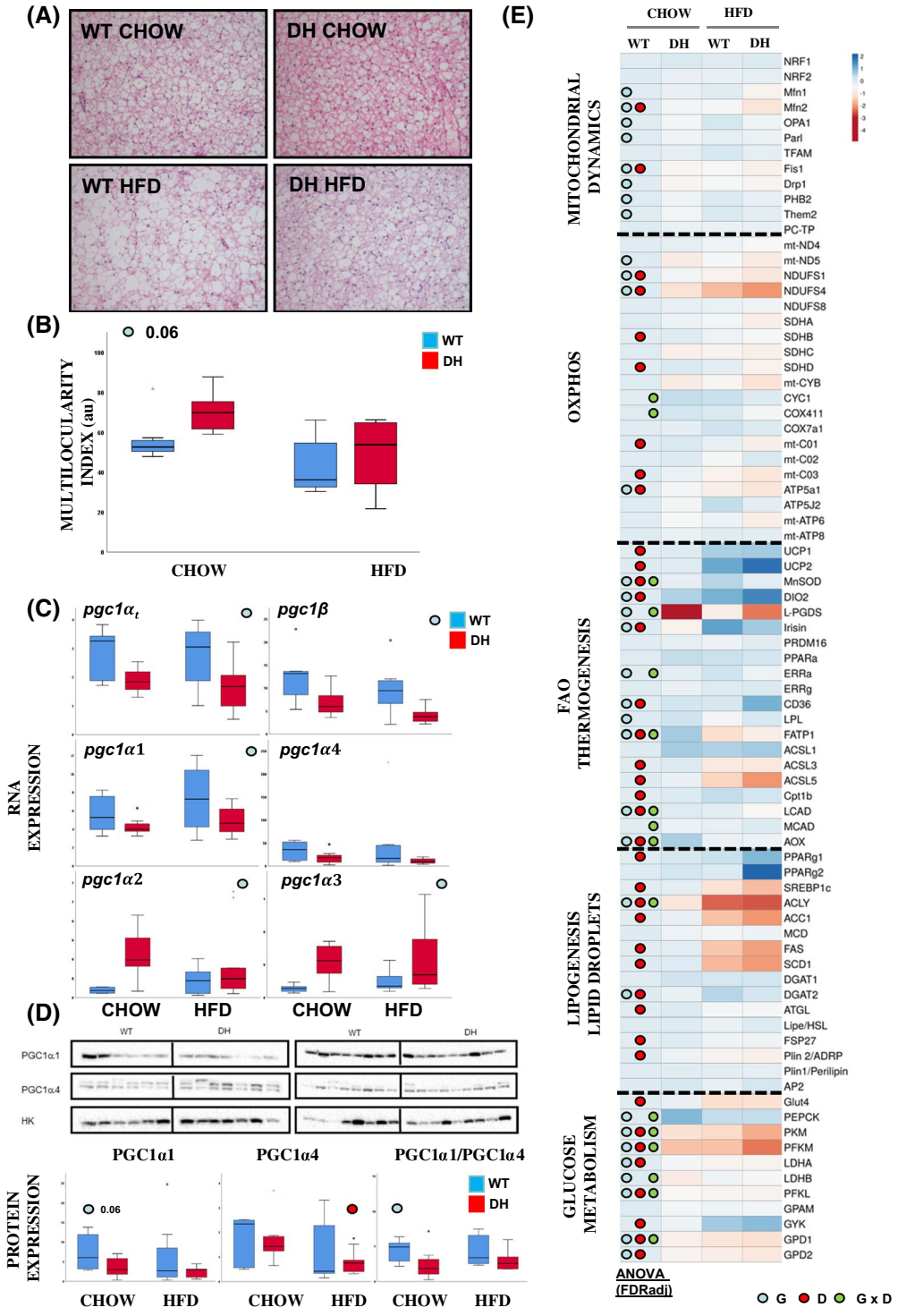

FIGURE 2 A, Representative histological sections (×10) of brown adipose tissue (BAT) and (B) analysis of inverse locularity area. Data presented as mean ± SEM. DH, $Pgc1\alpha^{[het]} \times Pgc1\beta^{[het]}$; WT, wild-type $^*P < .05$ by Two-way ANOVA. C, mRNA of PGC1α and β variants represented as box plots (n = 7-9). D, Western blot images for PGC1a variants and its quantification represented as box plots (n = 7-9). 2-way ANOVA, statistical significance $^*P < .05$ blue circle (genotype effect), red circle (diet effect), green circle (interactive effect). DH, $Pgc1\alpha^{[het]} \times Pgc1\beta^{[het]}$; WT, wild-type. E, BAT gene expression represented as heatmap using log2 where 0 states for WT chow (normalized as 1) (n = 7-9). Two-way ANOVA: blue circle (genotype effect), red circle (diet effect), green circle (interactive effect) $P < .05$

tendency to increased levels of *pparα* ($P \leq .05$, FDR ≥ 0.05) and *fatp1* (Figure 3E).

Additional profiling indicated that gWAT from DH mice was metabolically more active. gWAT had increased expression of genes involved in de novo lipogenesis and TG biosynthesis (eg, *acc1, gpam*), lipolysis (*atgl*) and glyceroneogenesis (eg, *pepck/pck1*) (Figure 3E). Similar to BAT, gene expression differences in gWAT were attenuated in DH mice-fed HFD. The profiling of macrophage markers in gWAT (Figure 3E)

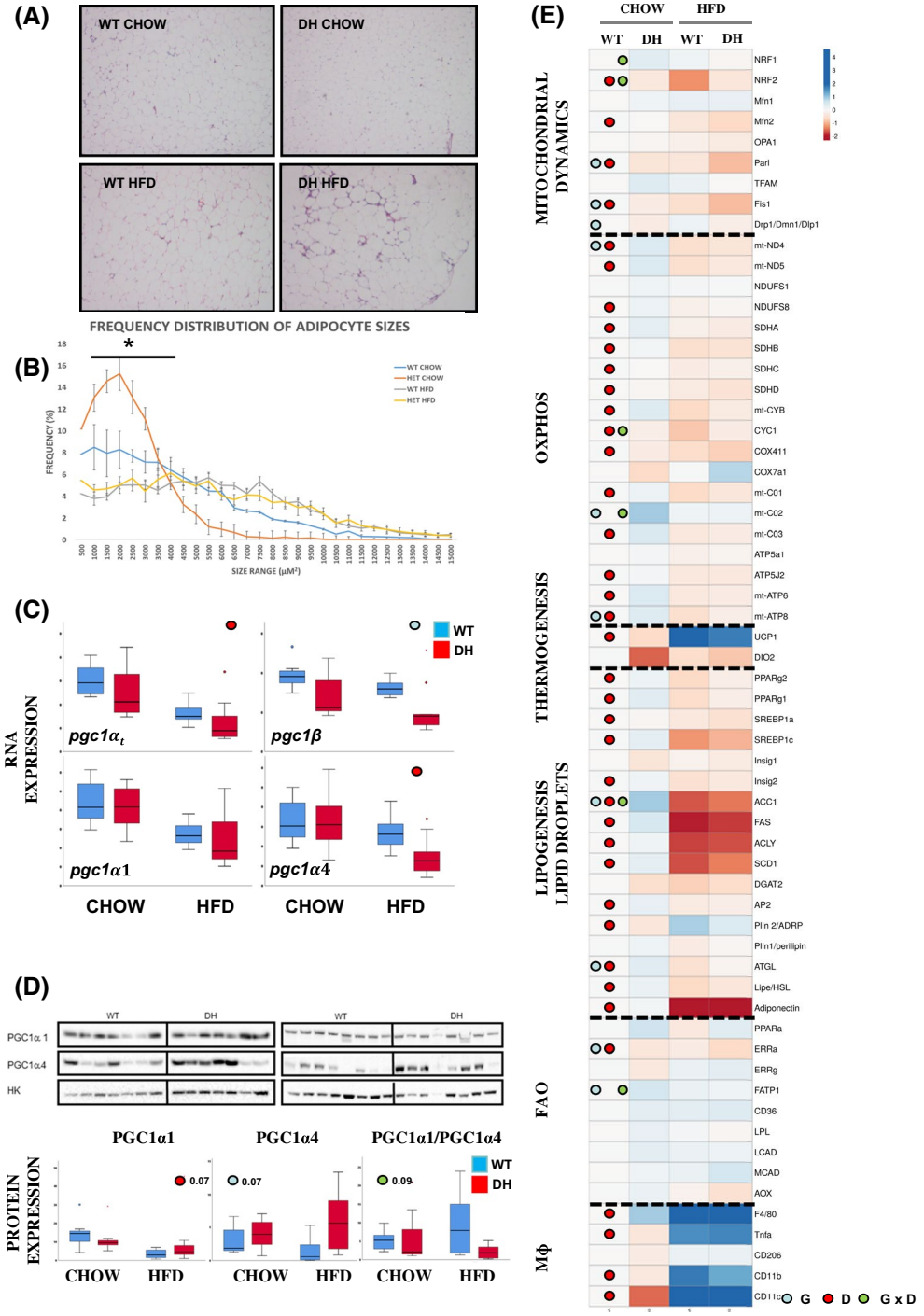

FIGURE 3 A, Representative histological sections (×10) of gWAT and (B) frequency distribution of adipocytes sizes (n = 7-9 mice per genotype). Data presented as mean ± SEM. DH, *Pgc1α*[het] × *Pgc1β*[het]; WT, wild-type *$P < .05$ by Two-way ANOVA. C, mRNA of PGC1α and β variants represented as box plots (n = 7-9). D, Western blot images for PGC1a variants and its quantification represented as box plots (n = 7-9). 2-way ANOVA, statistical significance *$P < .05$ blue circle (genotype effect), red circle (diet effect), green circle (interactive effect). DH, *Pgc1α*[het] × *Pgc1β*[het]; WT, wild-type. E, WAT gene expression represented as heatmap using log2 where 0 states for WT chow (normalized as 1) (n = 7-9). Two-way ANOVA: blue circle (genotype effect), red circle (diet effect), green circle (interactive effect) $P < .05$

revealed non-significant differences between genotypes. Therefore, the activation of both catabolic and anabolic pathways and the increase of mitochondrial machinery and pro-oxidative genes in gWAT from DH mice may be related to the partial allelic compensation of *pgc1α1* and increased levels of *pgc1α4*.

3.5 | The regulation of PGC1α1/PGC1α4 in the gastrocnemius muscle from *Pgc1α*[het] × *Pgc1β*[het] mice disrupts the expression of mitochondrial and myogenesis genes

PGC1α1 protein levels in gastrocnemius muscle depended on the interaction between genotype and diet being decreased levels in chow-fed DH and increased in HFD (Figure 4B). PGC1α4 levels tended to increase in DH so that the ratio of PGC1α1/PGC1α4 was decreased on chow and increased on HFD respectively, indicating specific nutritional regulation of each isoform.

Of note, both PGC1α2 and PGC1α3 mRNA were upregulated in the DH in both dietary conditions, whereas *pgc1β* mRNA levels were downregulated (Figure 4A).

In chow diet, this specific profile of PGC1α isoforms in DH mice was associated with decreased expression of several OXPHOS genes from complex 1 (eg, *ndufs1, ndufs4*) and *mfn1* (Figure 4C). On HFD, the ratio of PGC1α1/PGC1α4 was restored, and the differences attenuated. Further gene expression characterization found impaired upregulation of *slc25a25* mRNA and mild upregulation for phospholamban (*pnl)* in both chow and HFD fed DH indicating potential defects in calcium homeostasis and metabolic inefficiency (Figure 4C).

Profiling of metabolic genes in muscle revealed decreased levels of *fatp1, mcad,* and *pparα* in the DH muscle in chow-fed conditions indicative of impaired fatty acid uptake and oxidation ($P \leq .05$ FDR ≥ 0.05) (Figure 4C). Also, chow-fed DH mice exhibited a modest increase in myogenic markers *myh2* (oxidative IIa), *myh4* (glycolytic IIb), and *myh7* (oxidative type I) ($P \leq .05$ FDR ≥ 0.05), and increased levels of myogenic factors such as *follistatin*, as well as *myod*, *myf5,* and *myf6* ($P \leq .05$ FDR ≥ 0.05) (Figure 4C). No genotype associated differences were observed for GDF15.

On HFD, the muscle of DH mice also showed increased expression of myostatin, a cytokine that inhibits myogenesis. This is consistent with the decreased expression of PGC1α4 in HFD fed DH muscle derepressing myostatin.[6] Moreover, the diet-specific perturbation of PGC1α isoforms and PGC1β levels resulted in altered expression of myogenic factors. Despite mitochondrial and metabolic impairment in skeletal muscle no changes in the expression of *atrogin or murf1*, *suggestive* of atrophy were observed (Figure 4C).

3.6 | *Pgc1α*[het] × *Pgc1β*[het] mice had impaired hepatic FAO and de novo lipogenesis programs

The analysis of hepatic steatosis revealed a minor decrease in the hepatic fat content in the DH liver vs WT (Figure 5A,B). Hepatic protein levels of PGC1α1 and PGC1α4 were not different between genotypes (Figure 5D), despite their mRNA levels being decreased (Figure 5C).

Pgc1β mRNA in DH fed chow, or HFD was downregulated (Figure 5C). We also identified a specific subset of OXPHOS genes (*sdhd, cyc1, cox7a1*) (Figure 5E) and mitochondrial and peroxisomal FAO genes (eg, *abcd1, acca1, acot8, vlcad*) along with the stress-induced hormone *gdf15* whose expression was selectively impaired in DH mice (Figure 5E). These perturbations indicated that *pgc1β* specifically regulates these genes when PGC1 protein levels remain stable. Despite the decrease in the expression of FAO genes, the levels of hepatic acyl-carnitines were not different between genotypes (Figure S3D), suggesting that the hepatic β-oxidation program was effective in DH mice.

De novo *lipogenesis* gene expression was reduced in the livers of chow-fed DH (Figure 5E) as indicated by decreased *fas* and *scd1* levels, downregulation of *pparγ1/2 and srebp1*. The decreased expression of *irs*, *irs2* was a signature of hepatic insulin resistance (Figure 5E). Also, the increase in *pepck/pck1* in the fed state was in agreement with the phenotype of *pgc1α*^{KO}, and confirmed the existence of factors independent of PGC1αincreasing the expression of *pepck/pck1*.[4]

3.7 | *Pgc1α*[het] × *Pgc1β*[het] mouse livers show enrichment of unsaturated and long TG, increased SM, and decreased PC/PE ratio

Global Lipidomics revealed that the ethanolamine glycerophospholipids—containing both, ether (ePE) an ester bonds (PE) were increased in the livers of DH mice (Figure 6A and Figures S3B–S4A,C), decreasing the PC/PE and ePC/ePE ratios (Figure 6A). These lipid changes were not associated with changes in the expression of *etnk* (gene of the CDP-ethanolamine pathway), *pisd* (involved in the biosynthesis of PE, decarboxylation from PS to PE), or *pemt*, (conversion from PE to PC) (Figure 5E).

HFD increased TG content in both genotypes (Figure 6A). Chow-fed lean DH mice exhibited a small reduction in the hepatic TG content paralleling lower plasma TG.[22] Qualitative analysis of TG lipid composition revealed that chow-fed DH livers were enriched in TGs containing double bonds ($n \geq 3$) and carbons ($n \geq 53$), suggestive of an increased PUFAs/MUFA-TG ratio (Figures 6A, S1A and S2A). This fatty acid profile was consistent with increased expression of long fatty acid desaturases *fads1* and *2* ($P \leq .05$ FDR ≥ 0.05) as well as several elongases including *elovl5* and *6* (Figure 5E).

DAG profiling evidenced a strong genotype × diet interaction effect (Figure 6B). In chow-fed, DAGs were higher in DH vs WT. This pattern of DAGs was reversed on HFD. MANOVA revealed that this DAG fingerprint discriminated the genotypes (Figure 6A-C).

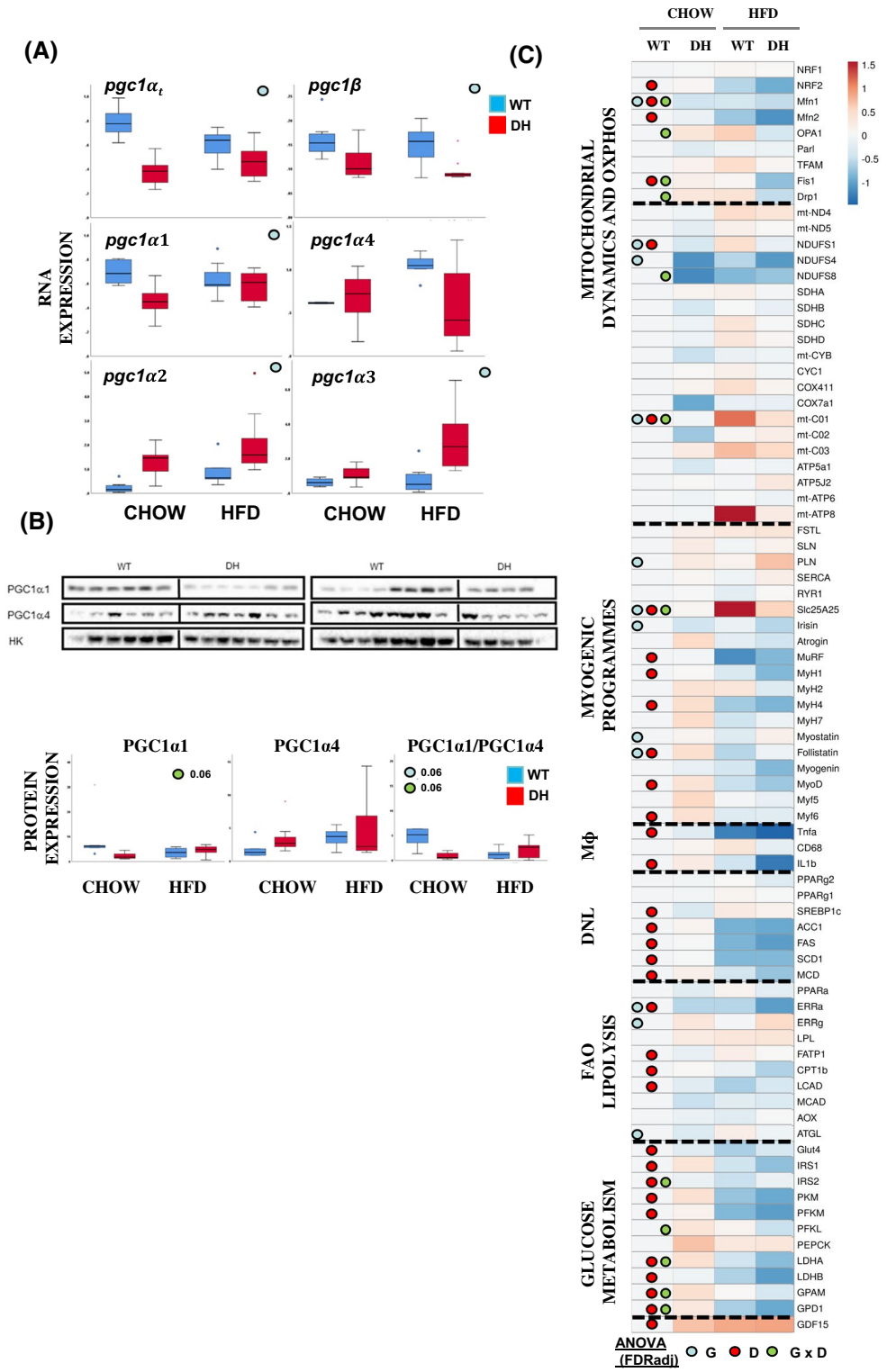

FIGURE 4 A, mRNA of PGC1α and β variants represented as box plots (n = 7-9). B, Western blot images for PGC1a variants and its quantification represented as box plots (n = 7-9). Two-way ANOVA, statistical significance $*P < .05$ blue circle (genotype effect), red circle (diet effect), green circle (interactive effect). DH, $Pgc1\alpha^{[het]} \times Pgc1\beta^{[het]}$; WT, wild-type. C, Gastrocnemius gene expression represented as heatmap using log2 where 0 states for WT chow (normalized as 1) (n = 7-9). Two-way ANOVA: blue circle (genotype effect), red circle (diet effect), green circle (interactive effect) $P < .05$

Ceramides were marginally increased in HFD vs chow-fed mice, although several species showed substantial significant changes (Figures 6A and S4B). This pattern reflects the increased flux of dietary palmitate due to the high fat intake diverted toward sphingolipid biosynthesis. Interestingly, the levels of sphingomyelins in DH were increased, both in

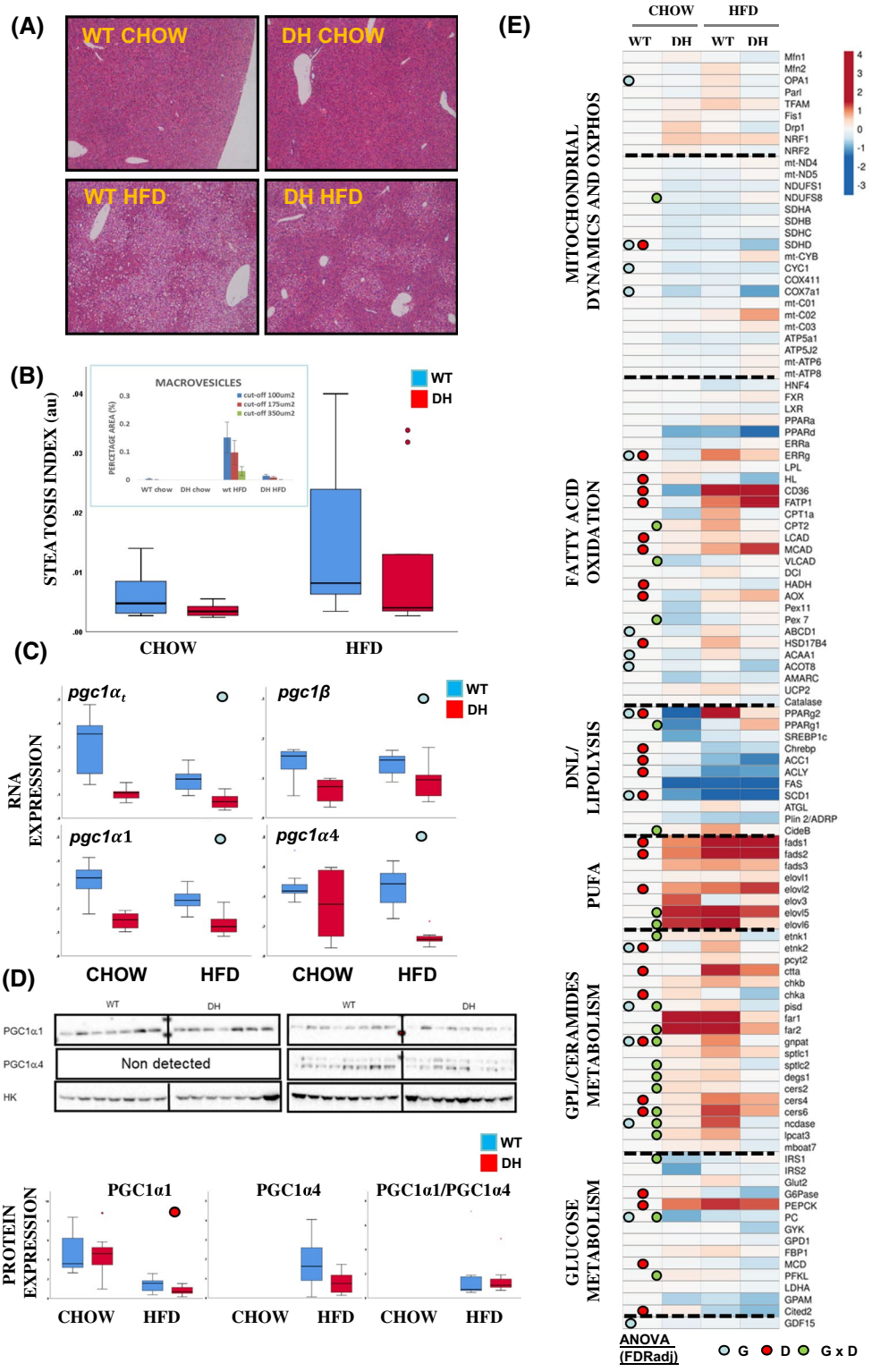

FIGURE 5 A, Representative histological sections (×10) of the liver and (B) analysis steatosis and presence of macrovesicles (n = 7-9 mice per genotype). Data presented as mean ± SEM. DH, $Pgc1\alpha^{[het]} \times Pgc1\beta^{[het]}$; WT, wild-type *$P < .05$ by Two-way ANOVA. C, mRNA of PGC1α and β variants represented as box plots (n = 7-9). D, Western blot images for PGC1a variants and its quantification represented as box plots (n = 7-9). Two-way ANOVA, statistical significance *$P < .05$ blue circle (genotype effect), red circle (diet effect), green circle (interactive effect). DH, $Pgc1\alpha^{[het]} \times Pgc1\beta^{[het]}$; WT, wild-type. E, Hepatic gene expression represented as heatmap using log2 where 0 states for WT chow (normalized as 1) (n = 7-9). Two-way ANOVA: blue circle (genotype effect), red circle (diet effect), green circle (interactive effect) $P < .05$

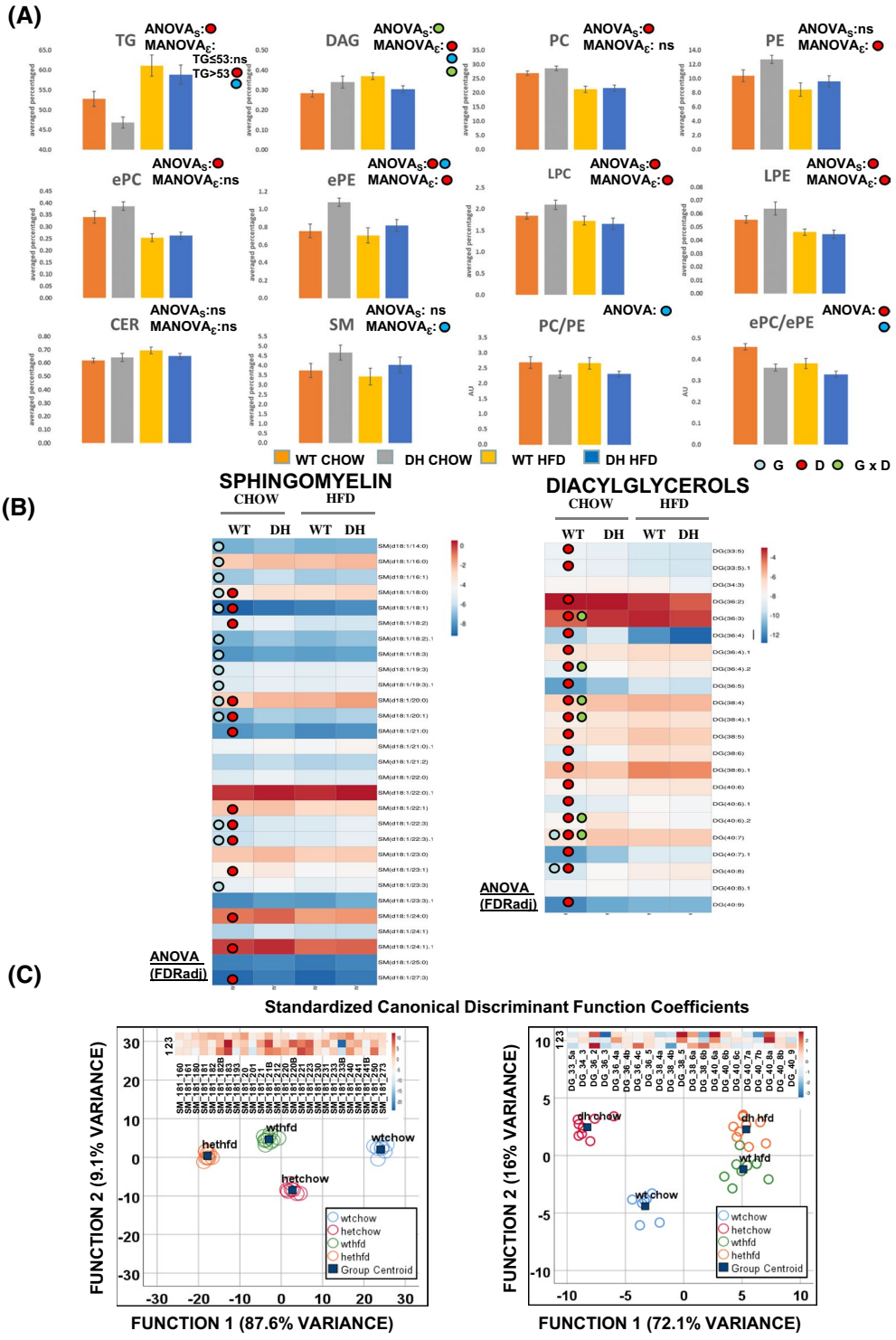

FIGURE 6 A, Lipidomic profiling represented as the average of percentages of the different lipid species in the liver from males WT and DH fed both chow and high-fat diet. Triacylglycerols (TG), diacylglycerols (DAGs), ceramides (CER), sphingomyelins (SM). Phosphatidylethanolamines (PE), Phosphatidylcholines (PC), lysophosphatidylethanolamines (LPE), LysoPhosphatidylcholines (LPC), ether-linked-Phosphatidylethanolamines (ePE), ether linked-Phosphatidylcholines (ePC). (n = 7-9). MANOVA and ANOVA: blue circle (genotype effect), red circle (diet effect), green circle (interactive effect) $P < .05$. B, Heatmaps of the independent lipid identities for Sphingomyelins and Diacylglycerols represented as heatmap using log2 of the % of the lipids (n = 7-9). ANOVA: blue circle (genotype effect), red circle (diet effect), green circle (interactive effect) $P < .05$. C, Group plots derived from the Discriminant Analysis and standardized canonical discriminant function coefficients for SM and DAG are shown

fed chow and HFD in comparison to WT mice (Figure 6A). MANOVA revealed that SM composition provided a unique fingerprint for the discrimination of WT and DH groups independently of the diet (Figure 6A-C). These lipid patterns suggested that the sphingolipid rheostat was modulated directly by *pgc1β* heterozygosity.

4 | DISCUSSION

Here, we investigated whether partial genetic ablation of *pgc1α* and *pgc1β*, as observed in the elder, obese and diabetic patients, act as "primary movers" in the pathogenesis of metabolic disease. We hypothesized that dysregulation of both PGC1α and PGC1β would link obesity and insulin resistance in a context of positive energy balance (HFD). The phenotype of global *pgc1α/pgc1β*^{DKO} mouse has shown that simultaneous absence of *pgc1α* and *pgc1β* causes a severe mitochondrial phenotype and early lethality.[32] Our model aimed to be more pathophysiologically relevant by engineering a milder dysregulation of both PGC1s, recapitulating the changes of obesity and T2DM. We posited that the DH mouse would provide new insights on the bioenergetic and metabolic defects associated with obesity, T2DM and aging and define a hierarchical organ-specific contribution to metabolic stress during the natural history of the disease.

Contrary to our initial hypothesis, the metabolic characterization of the DH model showed a lean, insulin-sensitive mouse with increased EE when fed chow. This advantageous metabolic phenotype was partially neutralized in DH mice fed on HFD. On chow, DH mice were hypermetabolic with a "metabolically healthy" phenotype characterized by decreased fat mass, smaller adipocytes, and improved insulin sensitivity. The chow-fed DH exhibited a lean phenotype resulting from increased BAT thermogenic activity. DH mice were not lipodystrophic, as they had decreased insulinemia (suggestive of improved insulin sensitivity), had a healthy adipose tissue and were able to gain weight when on HFD. This phenotype did not exclude defects in glucose-stimulated insulin secretion, whose adverse effects were likely to be obscured by improved peripheral glucose disposal or increased insulin clearance in liver and kidney. This healthy metabolic phenotype resembled aspects of the *pgc1β*^{KO} in terms of leanness, increased EE and thermogenic capacity at RT and shared similarities with the lean phenotype observed in the *pgc1α*^{KO}.[4] Thus, the DH model clashed with the current view that defective PGC1s causing mitochondria dysfunction promote insulin resistance/diabetes. We rationalized that the DH mouse may represent an early stage of the metabolic adaptations aimed to maintain homeostasis.

The analysis of the DH mouse provides unique insights. We show that specific nutrients regulate gene expression and PGC1α1 and PGC1α4 protein isoforms in vivo in a tissue-specific pattern. The organ-specific changes observed in PGC1α isoforms may have been influenced by inter-organ compensatory crosstalks attempting to buffer the dysfunction of the more severely affected organs. Our data also confirm that *pgc1β*, at least at mRNA level, is not subjected to homeostatic regulation as its expression is decreased in all the DH tissues independently of the nutritional challenge.

Analysis of BAT from DH showed a consistent heterozygous profile for *pgc1*β, and PGC1α1 and PGC1α4 isoforms coupled to downregulation of mitochondrial genes. Despite this, DH BAT was more multilocular than WT mice, had increased in *dio2* mRNA levels, suggestive of increased SNS tone, and high expression of genes involved in FAO. We speculate that BAT may have increased or switched fuels as a result of inefficient mitochondrial performance. In this line, recent investigations have shown that imbalance of the components of OXPHOS machinery in BAT promotes metabolic benefits at the expense of its adaptive thermogenic function.[35] It is also possible that the increased expression of PGC1α2 and α3 may have contributed to this paradoxical phenotype. The relevance of those isoforms in adaptive thermogenesis remains unexplored.

The expression of PGC1α1 in skeletal muscle of DH mice was decreased and associated with impaired expression of mitochondrial, fiber types and myogenesis-related genes. This phenotype was reminiscent of the muscle-specific *pgc1α/β*^{DKO} with alterations in OXPHOS, impaired expression of fibers remodeling and FAO genes and where the overexpression of ERRγ reinstated mitochondrial bioenergetics.[36-38] Of note the *errγ/erra* ratio was increased in the DH muscle, which we interpret as an allostatic attempt to restore adequate muscle function.

The DH muscle had upregulation of PGC1α4—the isoform with higher protein stability.[5] Both PGC1α1 and PGC1α4 isoforms have distinctive roles, either regulating OXPHOS or promoting hypertrophic muscle programs, respectively.[6,39] The upregulation of PGC1α2 and PGC1α3[5] emphasizes the importance of the coordination of *pgc1α* and its variants with *pgc1β* for muscle homeostasis. Whereas these alterations have not resulted in significant changes in gene expression, they have determined an unexpected improvement in carbohydrate metabolism.

Global lipidomics revealed a unique fingerprint in the livers of DH mice defined by changes in the PC/PE ratio, TG, DAG and SM composition. Decreased PC/PE and/or increased levels of PE are characteristic of NASH in mice and patients.[40-42] Changes in PC/PEs affect biophysical properties of cellular membranes, increase mitochondrial respiration and NAFLD—as seen in the *pemt*^{KO}—.[43,44] Increased levels of hepatic SM are also associated with pro-atherogenic risk in rodent models.[45] Whether the lipidome of DH mice suffices to increase the susceptibility to NAFLD and/or associated metabolic complications will require further research.

Analysis of DH WAT showed maintained expression of PGC1α1 and increased PGC1α4 vs WT. This was reminiscent of the upregulation of PGC1α in *pgc1β*^{KO} WAT.[22,46] The upregulation of PGC1α4 in DH WAT was associated with a transcriptional signature reminiscent of activation of futile cycles and paradoxical increase of mitochondrially encoded OXPHOS genes. The increased mt-OXPHOS/nt-OXPHOS expression linked to increased levels of PGC1α has been previously associated with a "browning" phenotype in white adipocytes under nutrient/caloric restriction.[47,48] The emerging critical question is why obese and diabetic patients fail to activate these allostatic responses WAT. This adaptive failure to respond may be a novel lead to understand the metabolic maladaptation in these patients.

The DH mice hypermetabolic and improved carbohydrate metabolism was unexpected. The DH mouse was a healthy lean mouse despite having mitochondrial dysfunction in vital metabolic organs. In our opinion, the beneficial phenotype of the DH mice—in terms of energy balance—may have been promoted by the transient compensation of PGC1α4 protein levels in WAT. This robust allostatic response, increased thermogenesis in BAT facilitating carbohydrate utilization in the context of mitochondrial dysfunction and reduced PGC1 levels. Nevertheless, we cannot discard the potential contribution of other peripheral organs to this hypermetabolic phenotype as a result of the activation of futile cycles independent of mitochondrial performance.

Despite these metabolic advantages, defective PGC1α and PGC1β dysregulated the myogenic program and disrupted the hepatic lipidome. These changes may increase the susceptibility to muscle sarcopenia and NASH, both typically seen in diabetes and obesity.

An exciting concept emerging from this and previous work with the *pgc1β*^{KO} [22] is that defects in PGC1 and associated mitochondrial dysfunction may not be the primary cause of insulin resistance/diabetes. Useful to reconcile this apparent paradox is the concept of allostasis, referred to adaptive responses to maintain homeostasis at the expense of an allostatic load, or metabolic stress in this context, ultimately leading to the failure of the system. This allostatic concept is useful to understand other models of primary mitochondrial derangements "paradoxically" associated with beneficial metabolic effects as observed in the *tfam* WAT KO and muscle KO also characterized by remodeling of OXPHOS, increased ETC flux and mitochondrial uncoupling[49,50] A priori, these and other studies raise the possibility that decreasing mitochondrial function in muscle and or adipose tissue can protect from obesity associated comborbidities such as insulin resistance or even extend lifespan. However, they must be interpreted with some caution as the phenotype might respond to a transient activation of a variety of compensatory mechanisms that will eventually fail. In this regard, our gene profiling refutes GDF15—a stress response hormone linked to mitochondrial dysfunction that has recently emerged as a relevant player in energy balance[51]—acting as an adaptive mechanism to preserve health in the DH mice.

We hypothesize that in our DH model, the activation of allostatic adaptations to metabolic stressors might enhance mitochondrial functionality in WAT when other highly metabolic organs are compromised. The subsequent failure of these allostatic mechanisms in response to a mounting allostatic load, typically in the aged patient, maybe the final trigger unmasking the severity of a metabolic phenotype. Unfortunately, no studies have been designed yet to unmask the long-term effects and the mechanisms controlling the initiation and failure of allostatic mechanisms acting in mitochondrial dysfunction models.

ACKNOWLEDGMENTS

This work was funded by FP7-MITIN [HEALTH-F4-2008-223450] and the MRC MDU [MC_UU_12012/2]. SRC was also funded by MEIF-CT-2005-023061. The Biochemistry Assay Lab and the Histopathology Core are funded by MRC Metabolic Diseases Unit [MC_UU_00014/5]; Imaging Core is funded by Wellcome Trust Major Award [208363/Z/17/Z].

CONFLICT OF INTEREST

The authors declare that they have no conflict of interest. MB, MB-Y, and DL are AstraZeneca employees.

AUTHOR CONTRIBUTIONS

S. Rodriguez-Cuenca and C.J. Lelliot conceived the original hypothesis, designed and performed experiments in vivo/ex vivo and wrote the manuscript; G. Peddinti, T. Hyötyläinen, and M. Orešič performed the lipid composition analysis in the liver, discussed, and edited the manuscript; M. Campbell, A. Rita Dias, J. Relat, S. Mora, M. Martinez-Uña, and C. Ingvorsen contributed to ex vivo profiling, discussed, and edited the manuscript; M. Bjursell, M. Bohlooly-Y, and D. Lindén, conceived the original hypothesis, designed experiments, and edited the manuscript; A. Zorzano and A. Vidal-Puig, conceived the original hypothesis, designed experiments, and wrote the manuscript; S. Rodriguez-Cuenca, C.J. Lelliot, and A. Vidal-Puig are the guarantors of this work. All authors approved its publication.

ORCID

Sergio Rodriguez-Cuenca https://orcid.org/0000-0001-9635-0504

REFERENCES

1. Andersson U, Scarpulla RC. Pgc-1-related coactivator, a novel, serum-inducible coactivator of nuclear respiratory factor 1-dependent transcription in mammalian cells. *Mol Cell Biol*. 2001;21:3738-3749.

2. Arany Z, He H, Lin J, et al. Transcriptional coactivator PGC-1 alpha controls the energy state and contractile function of cardiac muscle. *Cell Metab*. 2005;1:259-271.
3. Lelliott CJ, Ljungberg A, Ahnmark A, et al. Hepatic PGC-1beta overexpression induces combined hyperlipidemia and modulates the response to PPARalpha activation. *Arterioscler Thromb Vasc Biol*. 2007;27:2707-2713.
4. Lin J, Wu PH, Tarr PT, et al. Defects in adaptive energy metabolism with CNS-linked hyperactivity in PGC-1alpha null mice. *Cell*. 2004;119:121-135.
5. Martinez-Redondo V, Jannig PR, Correia JC, et al. Peroxisome proliferator-activated receptor gamma coactivator-1 alpha isoforms selectively regulate multiple splicing events on target genes. *J Biol Chem*. 2016;291:15169-15184.
6. Ruas JL, White JP, Rao RR, et al. A PGC-1alpha isoform induced by resistance training regulates skeletal muscle hypertrophy. *Cell*. 2012;151:1319-1331.
7. Vandenbeek R, Khan NP, Estall JL. Linking metabolic disease with the PGC-1alpha Gly482Ser polymorphism. *Endocrinology*. 2018;159:853-865.
8. Villegas R, Williams SM, Gao YT, et al. Genetic variation in the peroxisome proliferator-activated receptor (PPAR) and peroxisome proliferator-activated receptor gamma co-activator 1 (PGC1) gene families and type 2 diabetes. *Ann Hum Genet*. 2014;78:23-32.
9. Xia W, Chen N, Peng W, et al. Systematic meta-analysis revealed an association of PGC-1alpha rs8192678 polymorphism in type 2 diabetes mellitus. *Dis Markers*. 2019;2019:2970401.
10. Hernandez-Alvarez MI, Thabit H, Burns N, et al. Subjects with early-onset type 2 diabetes show defective activation of the skeletal muscle PGC-1{alpha}/Mitofusin-2 regulatory pathway in response to physical activity. *Diabetes Care*. 2010;33:645-651.
11. Mensink M, Hesselink MK, Russell AP, Schaart G, Sels JP, Schrauwen P. Improved skeletal muscle oxidative enzyme activity and restoration of PGC-1 alpha and PPAR beta/delta gene expression upon rosiglitazone treatment in obese patients with type 2 diabetes mellitus. *Int J Obes*. 2007;31:1302-1310.
12. Mootha VK, Lindgren CM, Eriksson KF, et al. PGC-1alpha-responsive genes involved in oxidative phosphorylation are coordinately downregulated in human diabetes. *Nat Genet*. 2003;34:267-273.
13. Bombassaro B, Ignacio-Souza LM, Nunez CE, et al. A20 deubiquitinase controls PGC-1alpha expression in the adipose tissue. *Lipids Health Dis*. 2018;17:90–100.
14. Heinonen S, Muniandy M, Buzkova J, et al. Mitochondria-related transcriptional signature is downregulated in adipocytes in obesity: a study of young healthy MZ twins. *Diabetologia*. 2017;60:169-181.
15. Moreno-Santos I, Perez-Belmonte LM, Macias-Gonzalez M, et al. Type 2 diabetes is associated with decreased PGC1alpha expression in epicardial adipose tissue of patients with coronary artery disease. *J Transl Med*. 2016;14:243–251.
16. Heinonen S, Buzkova J, Muniandy M, et al. Impaired mitochondrial biogenesis in adipose tissue in acquired obesity. *Diabetes*. 2015;64:3135-3145.
17. Kelstrup L, Hjort L, Houshmand-Oeregaard A, et al. Gene expression and DNA methylation of PPARGC1A in muscle and adipose tissue from adult offspring of women with diabetes in pregnancy. *Diabetes*. 2016;65:2900-2910.
18. Pellegrinelli V, Rouault C, Rodriguez-Cuenca S, et al. Human adipocytes induce inflammation and atrophy in muscle cells during obesity. *Diabetes*. 2015;64:3121-3134.
19. Ling C, Poulsen P, Carlsson E, et al. Multiple environmental and genetic factors influence skeletal muscle PGC-1alpha and PGC-1beta gene expression in twins. *J Clin Invest*. 2004;114:1518-1526.
20. Patti ME, Butte AJ, Crunkhorn S, et al. Coordinated reduction of genes of oxidative metabolism in humans with insulin resistance and diabetes: potential role of PGC1 and NRF1. *Proc Natl Acad Sci U S A*. 2003;100:8466-8471.
21. Besse-Patin A, Leveille M, Oropeza D, Nguyen BN, Prat A, Estall JL. Estrogen signals through peroxisome proliferator-activated receptor-gamma coactivator 1alpha to reduce oxidative damage associated with diet-induced fatty liver disease. *Gastroenterology*. 2017;152:243-256.
22. Lelliott CJ, Medina-Gomez G, Petrovic N, et al. Ablation of PGC-1beta results in defective mitochondrial activity, thermogenesis, hepatic function, and cardiac performance. *PLoS Biol*. 2006;4:e369.
23. Sczelecki S, Besse-Patin A, Abboud A, et al. Loss of Pgc-1alpha expression in aging mouse muscle potentiates glucose intolerance and systemic inflammation. *Am J Physiol Endocrinol Metab*. 2014;306:E157-E167.
24. Sonoda J, Mehl IR, Chong LW, Nofsinger RR, Evans RM. PGC-1beta controls mitochondrial metabolism to modulate circadian activity, adaptive thermogenesis, and hepatic steatosis. *Proc Natl Acad Sci U S A*. 2007;104:5223-5228.
25. D'Errico I, Salvatore L, Murzilli S, et al. Peroxisome proliferator-activated receptor-gamma coactivator 1-alpha (PGC1alpha) is a metabolic regulator of intestinal epithelial cell fate. *Proc Natl Acad Sci U S A*. 2011;108:6603-6608.
26. Rodriguez-Cuenca S, Carobbio S, Barcelo-Coblijn G, et al. P465L-PPARgamma mutation confers partial resistance to the hypolipidaemic action of fibrates. *Diabetes Obes Metab*. 2018;20:2339-2350.
27. Nelson W, Tong YL, Lee JK, Halberg F. Methods for cosinor-rhythmometry. *Chronobiologia*. 1979;6:305-323.
28. Medina-Gomez G, Yetukuri L, Velagapudi V, et al. Adaptation and failure of pancreatic beta cells in murine models with different degrees of metabolic syndrome. *Dis Model Mech*. 2009;2:582-592.
29. Pluskal T, Castillo S, Villar-Briones A, Oresic M. MZmine 2: modular framework for processing, visualizing, and analyzing mass spectrometry-based molecular profile data. *BMC Bioinform*. 2010;11:395.
30. Tschop MH, Speakman JR, Arch JR, et al. A guide to analysis of mouse energy metabolism. *Nat Methods*. 2011;9:57-63.
31. Molenaar MR, Jeucken A, Wassenaar TA, van de Lest CHA, Brouwers JF, Helms JB. LION/web: a web-based ontology enrichment tool for lipidomic data analysis. *Gigascience*. 2019;8, 1–10.
32. Lai L, Leone TC, Zechner C, et al. Transcriptional coactivators PGC-1alpha and PGC-lbeta control overlapping programs required for perinatal maturation of the heart. *Genes Dev*. 2008;22:1948-1961.
33. Virtue S, Feldmann H, Christian M, et al. A new role for lipocalin prostaglandin d synthase in the regulation of brown adipose tissue substrate utilization. *Diabetes*. 2012;61:3139-3147.
34. Ellis JM, Li LO, Wu PC, et al. Adipose acyl-CoA synthetase-1 directs fatty acids toward beta-oxidation and is required for cold thermogenesis. *Cell Metab*. 2010;12:53-64.
35. Masand R, Paulo E, Wu D, et al. Proteome imbalance of mitochondrial electron transport chain in brown adipocytes leads to metabolic benefits. *Cell Metab*. 2018;27:616-629.e4.
36. Fan W, He N, Lin CS, et al. ERRgamma promotes angiogenesis, mitochondrial biogenesis, and oxidative remodeling in PGC1alpha/beta-deficient muscle. *Cell Rep*. 2018;22:2521-2529.

37. Rowe GC, Patten IS, Zsengeller ZK, et al. Disconnecting mitochondrial content from respiratory chain capacity in PGC-1-deficient skeletal muscle. *Cell Rep*. 2013;3:1449-1456.
38. Zechner C, Lai L, Zechner JF, et al. Total skeletal muscle PGC-1 deficiency uncouples mitochondrial derangements from fiber type determination and insulin sensitivity. *Cell Metab*. 2010;12:633-642.
39. Martinez-Redondo V, Pettersson AT, Ruas JL. The hitchhiker's guide to PGC-1alpha isoform structure and biological functions. *Diabetologia*. 2015;58:1969-1977.
40. Arendt BM, Ma DW, Simons B, et al. Nonalcoholic fatty liver disease is associated with lower hepatic and erythrocyte ratios of phosphatidylcholine to phosphatidylethanolamine. *Appl Physiol Nutr Metab*. 2013;38:334-340.
41. Li Z, Agellon LB, Allen TM, et al. The ratio of phosphatidylcholine to phosphatidylethanolamine influences membrane integrity and steatohepatitis. *Cell Metab*. 2006;3:321-331.
42. Nakatsuka A, Matsuyama M, Yamaguchi S, et al. Insufficiency of phosphatidylethanolamine N-methyltransferase is risk for lean non-alcoholic steatohepatitis. *Sci Rep*. 2016;6:21721.
43. Baker CD, Basu Ball W, Pryce EN, Gohil VM. Specific requirements of nonbilayer phospholipids in mitochondrial respiratory chain function and formation. *Mol Biol Cell*. 2016;27:2161-2171.
44. van der Veen JN, Lingrell S, da Silva RP, Jacobs RL, Vance DE. The concentration of phosphatidylethanolamine in mitochondria can modulate ATP production and glucose metabolism in mice. *Diabetes*. 2014;63:2620-2630.
45. Liu J, Zhang H, Li Z, et al. Sphingomyelin synthase 2 is one of the determinants for plasma and liver sphingomyelin levels in mice. *Arterioscler Thromb Vasc Biol*. 2009;29:850-856.
46. Zhai N, Sun C, Gu W, et al. Resistance to high-fat diet-induced obesity in male heterozygous Pprc1 knockout mice. *Endocr J*. 2015;62:633-644.
47. Lettieri Barbato D, Tatulli G, Aquilano K, Ciriolo MR. Mitochondrial Hormesis links nutrient restriction to improved metabolism in fat cell. *Aging*. 2015;7:869-881.
48. Lopez-Lluch G, Hunt N, Jones B, et al. Calorie restriction induces mitochondrial biogenesis and bioenergetic efficiency. *Proc Natl Acad Sci U S A*. 2006;103:1768-1773.
49. Vernochet C, Mourier A, Bezy O, et al. Adipose-specific deletion of TFAM increases mitochondrial oxidation and protects mice against obesity and insulin resistance. *Cell Metab*. 2012;16:765-776.
50. Wredenberg A, Freyer C, Sandstrom ME, et al. Respiratory chain dysfunction in skeletal muscle does not cause insulin resistance. *Biochem Biophys Res Commun*. 2006;350:202-207.
51. Breit SN, Brown DA, Tsai VW. The GDF15-GFRAL pathway in health and metabolic disease: friend or foe? *Annu Rev Physiol*. 2021;83:127-151.

SUPPORTING INFORMATION

Additional Supporting Information may be found online in the Supporting Information section.

How to cite this article: Rodriguez-Cuenca S, Lelliot CJ, Campbell M, et al. Allostatic hypermetabolic response in PGC1α/β heterozygote mouse despite mitochondrial defects. *The FASEB Journal*. 2021;35:e21752. https://doi.org/10.1096/fj.202100262RR